Journal of Research of the National Bureau of Standards Vol. 58, No. 2, February 1957 Research Paper 2736

Classification of Perovskite and Other ABO_3-Type Compounds[1]

Robert S. Roth

A classification of $A^{+2}B^{+4}O_3$ compounds has been made on the basis of ionic radii of the constituent ions. A graph of this type for the perovskite compounds can be divided into orthorhombic, pseudocubic, and cubic fields, with an area of ferroelectric and antiferroelectric compounds superimposed on the cubic field. The structures of solid solutions between various perovskite compounds cannot be completely correlated on the basis of this simple two-dimensional chart. Therefore, a new type of classification of the perovskite-type compounds has been attempted, using a three-dimensional graph with polarizability of ions plotted as the third dimension. This three-dimensional graph has been applied successfully to compounds of the type $A^{+2}B^{+4}O_3$, which crystallize with perovskite-type structures. In addition, a classification of double oxides of trivalent ions has shown that all compounds of this type having the perovskite structure can be divided into two groups, with rhombohedral and orthorhombic symmetry. No ideal cubic perovskites of the $A^{+3}B^{+3}O_3$ compounds have been found.

1. Introduction

A partial survey of the reactions occurring in binary oxide mixtures of the types $AO:BO_2$ and $A_2O_3:B_2O_3$ has been conducted as part of a program of fundamental research on ceramic dielectrics. In addition, binary, ternary, and quaternary reactions between end members of the $AO{\cdot}BO_2$ compounds have also been studied. Combinations of oxides giving the simple formula type ABO_3 were selected because of current interest in ferroelectric ceramics. Previous publications have covered the data compiled on many of these systems, such as CaO-TiO_2 [1],[2] $PbTiO_3$-$PbZrO_3$ [2], BeO with ZrO_2, TiO_2, and CeO_2 [3], MgO-CaO-SnO_2 and TiO_2 [4], MgO-ZrO_2-TiO_2 and CaO-ZrO_2-TiO_2 [5], alkaline earth oxides with GeO_2 [6], $PbTiO_3$-$PbZrO_3$-$PbO:SnO_2$ and $PbTiO_3$-$PbHfO_3$ [7], alkaline earth oxides with UO_2 [8], and divalent ions with ZrO_2 [9]. This paper is designed primarily to present new data and a new method of representation of these structure types and to coordinate the information already published.

2. Sample Preparations and Test Methods

In general the materials used were the highest available purity of the component oxides, varying from about 98.5- to 99.9-percent purity. The starting materials, in sufficient quantities to give either a 10.0-g sample or a 1.0-g sample, depending on the availability of the raw materials, were weighed to the nearest milligram, mixed together, and formed into 1-in. or ½-in.-diameter disks at a pressure of 5,000 lb/in.^{2} The pressed disks were fired for 4 hr at 1,100° C on platinum foil in an air atmosphere, using an electrically heated furnace wound with 80-percent-Pt 20-percent-Rh wire.

These disks were then ground and remixed, and new disks for study of the solid-state reactions, about ¼ in. high, were formed at 15,000 lb/in.^{2} in either a ½-in. or ¼-in.-diameter mold. The specimens were then fired in a conventional platinum-wound quench furnace, or refired in the original calcining furnace. The quenching technique was used, whenever applicable, because it has been observed that sharper X-ray patterns are often obtained by very fast cooling of the specimen. It is known that phase transitions in the perovskite structures are usually completely reversible and cannot be frozen in by quenching. Thus the perovskite structures discussed are the room-temperature stable forms, although other materials treated in this manner would generally contain the high-temperature forms, if any. The final firing temperature ranged from 1,250° to 1,550° C and was maintained constant for a given length of time. Equilibrium conditions were usually reached in less than 3 hr. Equilibrium was believed to have been reached when X-ray patterns of the specimen showed only a single phase or when the pattern of a multiple-phase specimen showed no change with successive heat treatment. The fired disks were examined by X-ray diffraction, using a Geiger-counter diffractometer employing nickel-filtered copper radiation. The X-ray data reported can be considered to be accurate to ± 0.001 A when three decimal places are recorded, and to ± 0.01 A° when only two decimal places are recorded. The results reported in this work are generally the data obtained at room temperature from specimens treated in a manner to form a matured ceramic dielectric body.

In the case of specimens containing an ion that was apt to oxidize, a neutral atmosphere was maintained in the furnace. These ions were V^{+4}, U^{+4}, and Ce^{+3}; the neutral atmosphere used was either helium or argon. The furnaces used were similar to those previously mentioned, but modified to maintain a neutral atmosphere.

3. The Perovskite Structure Type

The structures of the perovskite-type compounds have been studied by many workers. The exact nature of the structures involved is still in doubt in many cases. Conflicting reports in the literature make difficult the job of assigning the correct struc-

[1] This work has been sponsored as part of a program for Improvement of Piezoelectric Ceramics by the Office of Ordnance Research of the Department of the Army.

[2] Figures in brackets indicate the literature references at the end of this paper.

ture, or even symmetry, to any particular perovskite-type compound. The simplest case of the perovskite structure is that of a simple cubic cell with one ABX_3 formula unit per unit cell. In this case the A ions are at the corners of the unit cell with the B ion at the center and the negative ions occupying the face-centered positons. The space group is O_h^1-Pm3m and has the notation G–5 of the Strukturbericht [10]. As will be seen in the following discussion of actual perovskite-type compounds, very few binary oxides have this simple cubic structure at room temperature, although many of them assume this structure at elevated temperatures. Many modifications of this simple structure have been proposed to account for the X-ray patterns observed for different perovskite-type compounds. Among these modifications a simple doubling of the unit cell has been used [11]. A monoclinic modification suggested by Naray-Szabo [12] for the type compound perovskite ($CaTiO_3$) has been shown to be actually orthorhombic by Megaw [13]. The latest modification of this structure was made by Bailey [14] and quoted by Megaw [15], using an orthorhombic modification with the *b* parameter approximately twice the pseudocubic cell edge and with the *a* and *c* parameters approximately $\sqrt{2}$ times the pseudocubic cell. It will be seen that the X-ray patterns of a great many compounds can be indexed on the basis of this type of distortion of the perovskite structure. The compounds $CaTiO_3$, $CaZrO_3$, and $CaSnO_3$ have been indexed previously on this basis and the *d*-spacings and (*hkl*) values published [4, 5]. However, it should be noted that a discrepancy exists between the reported space group for $CaTiO_3$, Pcmn [15], and the published indexing of these patterns. Although $CaSnO_3$ contains no reflections that are not allowed by this space group, both $CaTiO_3$ itself and also $CaZrO_3$ show diffraction peaks, which can only be indexed on the basis of forbidden reflections. These peaks are especially prominent for $CaZrO_3$ and indicate that perhaps a different space group is required for the $CaTiO_3$-type orthorhombic modifications of the perovskite structure.

In addition to those types of distortions that require a multiplication of the pseudocubic cell, there are several other distortions in perovskite-type structures that require only a slight modification of one or two parameters, resulting in tetragonal, orthorhombic, and rhombohedral symmetries. It is these latter modifications that are of most interest in the study of ferroelectric forms of the perovskite structure, especially in the two groups of mixed oxides under discussion, $A^{+2}B^{+4}O_3$ and $A^{+3}B^{+3}O_3$. Other ferroelectric perovskite compounds, like $Na^{+1}Nb^{+5}O_3$, have been suggested to have multiple-type unit cells [16] even larger than in the $CaTiO_3$ type.

A classification of the perovskite-type structures on the basis of the radii of the constituent metallic ions has been attempted by several workers [17, 18, 16, 19]. It has been pointed out by Keith and Roy [19] that it is not advisable to attempt to classify more than one valence group of structure types on any one diagram. In other words, separate diagrams are needed for the compounds of the type $A^{+2}B^{+4}O_3$, $A^{+3}B^{+3}O_3$, $A^{+1}B^{+5}O_3$, etc. It seems quite probable that perovskite-type structures with F^{-1}, or some other such ion, in place of O^{-2} would also require separate diagrams for a reasonable classification. These diagrams still do not lend themselves to absolute classifications, as some compounds simply do not seem to fit. It has been suggested by Roberts [20, 21] that the polarization of the constituent ions may play an important role in determining the symmetry formed by a given pervoskite structure. A classic example of polarization determining crystal type over and above ionic radii may be found in the phenacite-olivine structure types where the Zn^{+2} ion is found to be out of place in a radii classification [22]. It is this notion of polarization that is used in the present paper in an attempt to make a better classification and diagrammatic representation of the perovskite structures.

4. Results and Discussion

4.1. Mixed Oxides of Divalent and Tetravalent Ions

a. General

For the purpose of convenience most of the data accumulated has been put in the form of tables, although some of the more controversial compositions are also discussed in the following sections. It is known that $CdTiO_3$ crystallizes in both the perovskite- and ilmenite-type structures [23]. As the perovskite structure requires a relatively large A ion and the ilmenite structure a relatively small A ion, it can be seen that all ABO_3 compounds with Ti^{+4} and an A^{+2} ion larger than Cd^{+2} should have the perovskite structure, whereas those with A^{+2} ions smaller than Cd^{+2} should have the ilmenite structure. In all such cases where compound formation takes place, this is found to be true. The values used in this study, for the radii of the metallic ions under consideration, are listed in table 1. The composition, structure type, and symmetry, where known, for the mixed oxides of divalent and tetravalent ions are listed in table 2. The parameters of the unit cell are given for all those materials studied. Information obtained in the present study is shown in bold-faced type, and the author's comments on previous work are given in italics. In general, references to other works are made only when the particular compound or mixture has not been studied in the present work or when results of other investigators disagree with the results found in the present investigation.

b. CeO_2:TiO_2

A specimen of CeO_2:TiO_2 heated in air has yielded an X-ray pattern of CeO_2 plus a perovskite-type phase. It seems highly unlikely that either CeO_2 or TiO_2 would reduce, in air, to the point of forming an $A^{+2}B^{+4}O_3$ structure. It seems more likely that an $A^{+3}B^{+3}O_3$ structure is the phase found in the X-ray pattern (see discussion of classification of mixed oxides of trivalent ions).

TABLE 1. *Radii and polarizability, where used, of metallic ions pertinent to this study*

Ion	Radius [a]	Polarizability [d]	Ion	Radius [a]
Divalent ions				
	A	*A*[3]		*A*
Ba^{+2}	1.34	70.6	Mn^{+2}	0.80
Pb^{+2}	1.20	91.8	Fe^{+2}	.74
Eu^{+2}	[b] 1.16	------	Zn^{+2}	.74
Sr^{+2}	1.12	49.1	Co^{+2}	.72
Ca^{+2}	0.99	34.9	Ni^{+2}	.69
Cd^{+2}	.97	[e] 56.9	Mg^{+2}	.66
			Be^{+2}	.35
Trivalent ions				
Al^{+3}	0.51	------	Bi^{+3}	0.96
Ga^{+3}	.62	------	Gd^{+3}	.97
Cr^{+3}	.63	------	Sm^{+3}	1.00
Fe^{+3}	.64	------	Nd^{+3}	1.04
Sc^{+3}	[c] .80	------	Ce^{+3}	1.07
In^{+3}	[c] .82	------	La^{+3}	1.14
Y^{+3}	.92	------	------	------
Tetravalent ions				
C^{+4}	0.16	------	Sn^{+4}	0.71
Si^{+4}	.42	------	Hf^{+4}	.78
Ge^{+4}	.53	------	Zr^{+4}	.79
Mn^{+4}	.60	------	Ce^{+4}	.94
V^{+4}	.63	------	U^{+4}	.97
Ti^{+4}	.68	------	Th^{+4}	1.02

[a] Unless otherwise indicated, radii of the ions are taken from Ahrens [30].

[b] The radius of Eu^{+2} has been adapted from the value given by Green [31] and corrected for radius of O^{-2}=1.40A.

[c] The radius of In^{+3} and Sc^{+3} are both given as 0.81 A by Ahrens [30]. As this cannot be shown on the diagram, In^{+3} is used as 0.82 A and Sc^{+3} as 0.80 A. This is thought to be justified as the compounds of Sc^{+3} are said to have slightly smaller parameters than the corresponding compounds of In^{+3} [19].

[d] Unless otherwise indicated, polarizability of the ions is taken from Roberts [20].

[e] The polarizability of Cd^{+2} was estimated as explained in text.

c. $SrZrO_3$

The compound $SrZrO_3$ has generally been regarded as a cubic perovskite [24, 16, 25]; although Naray-Szabo [26] has referred it, like $CaTiO_3$, to the monoclinic system. The X-ray pattern of this compound shows diffraction lines other than those found in simple cubic structures, definitely indicating some type of distortion of the unit cell. In addition, the "cubic" peaks in the $SrZrO_3$ pattern have a tendency to split into two or more peaks (not $K\alpha_1$ and $K\alpha_2$). The $K\alpha_2$ doublets cannot be clearly distinguished in the $SrZrO_3$ X-ray pattern, although they are quite clearly shown in patterns of the true cubic perovskite specimens like $BaZrO_3$ or $SrTiO_3$. The split in the pseudocubic peaks resembles those found in $PbZrO_3$ for a pseudotetragonal distortion with c/a 1, although there are a few possible discrepancies in intensity values. On the other hand, the distortion may be of the type found in $CaTiO_3$. As observed in at least six different specimens, the $SrZrO_3$ "pseudocubic" peak at a value of $h^2+k^2+l^2=6$ is split into a close doublet with the low-angle side of the doublet lower in intensity than the high-angle side. The same peak in $PbZrO_3$ has the intensities of the doublet reversed. Although $CaZrO_3$ and $CaTiO_3$ have four peaks very close together in this region, the two on the low-angle side are of lower intensity than the two on the high-angle side. Such discrepancies, noted above, make it impossible to assign $SrZrO_3$ to either the $PbZrO_3$ or $CaTiO_3$ structure. Calculations of *(hkl)* values for both types of cells, as well as theoretical intensity values for each structure, would have to be made before a final decision could be made.

TABLE 2. *Mixed oxides of the type* $A^{+2}B^{+4}O_3$

Composition	Tolerance factor for perovskite structure[a]	Heat treatment: Temperature (°C)	Heat treatment: Time (hr)	Structure type	Symmetry	References and discussion
Mixed oxides containing CO_2						
$BaCO_3$	------	------	------	Aragonite	Orthorhombic	Palache, Berman, and Frondel [39].
$PbCO_3$	------	------	------	do	do	Do.
$SrCO_3$	------	------	------	do	do	Do.
$CaCO_3$	------	------	------	do	do	Do.
$CaCO_3$	------	------	------	Calcite	Rhombohedral	Do.
$CdCO_3$	------	------	------	do	do	Do.
$MnCO_3$	------	------	------	do	do	Do.
$FeCO_3$	------	------	------	do	do	Do.
$ZnCO_3$	------	------	------	do	do	Do.
$CoCO_3$	------	------	------	do	do	Do.
$MgCO_3$	------	------	------	do	do	Do.
Mixed oxides containing SiO_2						
$BaSiO_3$	------	------	------	**Unknown**	------	**Present work.** *Specimen supplied by E. Levin of NBS staff.*
$PbSiO_3$	------	------	------	Unknown	------	Winchell [40].
$SrSiO_3$	------	------	------	**Pseudowollastonite**	**Unknown**	**Present work.** *Specimen supplied by E. T. Carlson of NBS staff.*
$CaSiO_3$	------	1,400	------	**Pseudowollastonite**	**Unknown**	**Present work.** *Specimen supplied by H. S. Yoder of Geophyscial Laboratory, Carnegie Inst., Washington, D. C.*
$CdSiO_3$	------	------	------	Unknown	------	Silverman, Morey, and Rossini [41].
$MgSiO_3$	------	------	------	**Enstatite**	**Orthorhombic**	**Present work.** *X-ray data obtained from specimen of Bishopsville meteorite supplied by H. S. Yoder. a=18.222, b=8.810, c=5.182 A.*

TABLE 2. *Mixed oxides of the type $A^{+2}B^{+4}O_3$*—Continued

Composition	Tolerance factor for perovskite structure[a]	Heat treatment: Temperature (°C)	Heat treatment: Time (hr)	Structure type	Symmetry	References and discussion
Mixed oxides containing GeO_2						
$BaGeO_3$	1.00	1,235	1	**Pseudowollastonite**	**Uknown**	**Roth** [6]. *Symmetry almost hexagonal.*
		700	1	**Pseudowollastonite**	**Unknown**	**Roth** [6]. *Heated at 20,000 psi.*
$PbGeO_3$	0.95	775	0.5	**Unknown**		**Present work.** *Probably nonequilibrium.*
$SrGeO_3$	.92	1,235	1	**Pseudowollastonite**	**Unknown**	**Roth** [6].
$CaGeO_3$	.88	1,235	1	**Unknown**		**Roth** [6]. *Probably nonequilibrium.*
$CdGeO_3$	.87	1,100	1	**Unknown**		**Present work.** *Probably nonequilibrium.*
$ZnO:GeO_2$	.78	1,100	0.66	**No 1:1 compound**		**Present work.** *Speciment contains* Zn_2GeO_4, *willemite type, plus* GeO_2, *quartz type.*
$MgGeO_3$	.75	1,235	1	**Enstatite**	**Orthorhombic**	**Roth** [6]. *a=18.661, b=8.954, c=5.346 A.*
$BeO:GeO_2$	.64			No information		*1:1 compound between* BeO *and* GeO_2 *seems unlikely; probably only* Be_2GeO_4 *forms.*
Mixed oxides containing MnO_2						
$CaMnO_3$[b]	0.84			Perovskite	Cubic	Ward, Gushee, McCarrol, and Ridgely [42].
				Perovskite	Cubic	Yakel [43]. Symmetry reported as cubic with doubled cell.
Mixed oxides containing VO_2						
$BaVO_3$	0.95	1,200 (**Helium**)	0.5	**Unknown**		**Present work.**
$SrVO_3$	.88	1,200 (**Helium**)	.5	**Unknown**		**Present work.**
$CaVO_3$	.83	1,300 (**Helium**)	.5	**Perovskite**	**Orthorhombic** [c]	**Present work.** *a=5.326, b=7.547, c=5.352 A.*
				Perovskite	Cubic	Ward, Gushee, McCarrol, and Ridgely [42].
$MgO:VO_2$	.72			Unknown		King and Suber [44].
$BeO:VO_2$	.61			Unknown		King and Suber [44].
Mixed oxides containing TiO_2						
$BaTiO_3$	0.93	1,350	2	**Perovskite**	**Tetragonal c/a>1**	**Present work.** *a=3.989, c=4.029 A.*
$PbTiO_3$	.88	1,100	1	**Perovskite**	**Tetragonal c/a>1**	**Jaffe, Roth, and Marzullo** [7]. *a=3.896, c=4.136 A.*
$EuTiO_3$	.87			Perovskite	Cubic	Brous, Fankuchen, and Banks [45].
$SrTiO_3$	.86	1,300	1	**Perovskite**	**Cubic**	**Present work.** *a=3.904 A.*
$CaTiO_3$	.81	>1,700	1.5	**Perovskite**	**Orthorhombic** [c]	**Coughanour, Roth, Marzullo, and Sennett** [4]. *a=5,381, b=7.645, c=5.443 A.*
$CdTiO_3$	.81	1,265	1	**Perovskite**	**Orthorhombic**	**Present work.** *a=5.301, b=7.606, c=5.419 A.*
$CdTiO_3$				Ilmenite	Rhombohedral	Posniak and Barth [23].
$MnTiO_3$	.75	1,250	1	**Ilmenite**	**Rhombohedral**	**Present work.** *a=5.585 A, α=54°57′.*
$FeTiO_3$	.73			Ilmenite	Rhombohedral	Wells [24].
$ZnO:TiO_2$	.73	1,245	1	**No 1:1 compound**		**Present work.** *Specimen contains* Zn_2TiO_4, *spinel type, plus* TiO_2, *rutile.*
$CoTiO_3$	.72	1,400	2	**Ilmenite**	**Rhombohedral**	**Present work.** *X-Ray pattern too diffuse to measure parameters.*
$NiTiO_3$	.71	1,400	2	**Ilmenite**	**Rhombohedral**	**Present work.** *a=5.448 A, α=55°.*
$MgTiO_3$	.70	1,550	2	**Ilmenite**	**Rhombohedral**	**Present work.** *a=5.519 A, α=54°30′.*
$BeO:TiO_2$	.60	1,800	0.5	**No reaction**		**Lang, Roth, and Fillmore** [3].
Mixed oxides containing SnO_2						
$BaSnO_3$	0.92	1,450	1	**Perovskite**	**Cubic**	**Present work.** *a=4.114 A.*
$PbO:SnO_2$	.87	850	1	**No 1:1 compound**		**Jaffe, Roth, and Marzullo** [7]. *Specimen contains* Pb_2SnO_4, *unknown structure plus* SnO_2.
		650	24	**No reaction**		*Starting material* PbO *and* SnO_2.
		650	0.5	**Unknown**		**Distorted fluorite-type structure, probably $PbSnO_4$.** *Starting material precipitated hydrated lead stannate.*
		800		$PbSnO_3$	Unknown	Coffen [46]. *Starting material precipitated hydrated lead stannate.*
				Perovskite	Tetragonal	Naray-Szabo [26].
$SrSnO_3$	.85			**Perovskite**	**Cubic**	**Present work.** *Commercial specimen, unfired. a=4.034 A.*
				Perovskite	Cubic	Megaw [13], Coffeen [46].
				Perovskite	$CaTiO_3$ type	Naray-Szabo [26].
$CaSnO_3$	.80	1,550	1	**Perovskite**	**Orthorhombic** [c]	**Coughanour, Roth, Marzullo, and Sennett** [4]. *a=5.518, b=7.884, c=5.564 A.*
$CdSnO_3$	.80	1,375	1	**No compound**		**Present work.** *Specimen contained only* SnO_2; CdO *volatilized. A compound of* $CdSnO_3$ *probably exists below this temperature.*
				Unknown		Coffeen [46]. *Decomposition of* $CdSnO_3$ *is about 1,177° C.*
				Perovskite	$CaTiO_3$ type	Naray-Szabo [26].
$MnO:SnO_2$	0.74	1,250	1	**No reaction**		**Present work.** MnO *added as* $MnCO_3$. *Specimen contained* SnO_2, Mn_3O_4.
$ZnSnO_3$ (?)	.72			Unknown		Coffeen [46]. *Published pattern probably spinel plus* SnO_2.
$CoO:SnO_2$	.71	1,300	1	**No 1:1 compound**		**Present work.** *Specimen contained* Co_2SnO_4, *spinel plus* SnO_2.
				Unknown		Coffeen [46]. *Published pattern that of a mixture of spinel and* SnO_2.

TABLE 2. *Mixed oxides of the type $A^{+2}B^{+4}O_3$*—Continued

Composition	Tolerance factor for perovskite structure[a]	Heat treatment: Temperature (°C)	Heat treatment: Time (hr)	Structure type	Symmetry	References and discussion
Mixed oxides containing SnO_2—Continued						
$NiSnO_3$	.70			Unknown		Coffeen [46].
$MgSnO_3$	.69	800	66	**Ilmenite**	**Rhombohedral**	**Coughanour, Roth, Marzullo, and Sennett** [4]. *X-ray pattern too diffuse to measure parameters.*
		1,000	48	**No 1:1 compound**		**Coughanour, Roth, Marzullo, and Sennett** [4]. *Specimen contains* Mg_2SnO_4, *spinel, plus* SnO_2.
		1,550	1	**No 1:1 compound**		**Coughanour, Roth, Marzullo, and Sennett** [4]. *Specimen contains* Mg_2SnO_4, *spinel, plus* SnO_2.
		816		Unknown		Coffeen [46].
$BeO:SnO_2$	.59					*No studies reported. Reaction unlikely from analogy to* BeO *systems.*
Mixed oxides containing HfO_2[d]						
$PbHfO_3$	0.84			Perovskite	Pseudotetragonal[e]	Shirane and Pepinsky [47].
$SrHfO_3$	.82			Perovskite	$CaTiO_3$ type	Naray-Szabo [26]. *Unlikely that pure* HfO_2 *was available at this time.*
$CaHfO_3$	78			Perovskite	$CaZrO_3$ type	Curtis, Doney, and Johnson [48].
Mixed oxides containing ZrO_2[f]						
$BaZrO_3$	0.88	1,450	1	**Perosvkite**	**Cubic**	**Present work.** *a=4.192 A.*
$PbZrO_3$	.84	1,350	1	**Perovskite**	**Pseudotetragonal**	**Jaffe, Roth, and Marzullo** [7]. *a=4.156, c=4.190 A.*
				Perovskite	Pseudotetragonal	Sawaguchi, Maniwa, and Hoshino [49].
				Perovskite	Pseudotetragonal	Sawaguchi, Shirane, and Takagi [50].[g]
$SrZrO_3$	.81	1,750	1	**Perosvkite**	**Pseudocubic**	**Present work.** *a=4.099 A. Starting material commercial* $SrZrO_3$, *also contains excess Monoclinic* ZrO_2 *plus unknown phase.*
		1,500	2	**Perovskite**	**Probably orthorhombic.**[c]	**Present work.** *a=5.792, b=8.189, c=5.818 A. Starting material* $SrCO_3$ *plus Monoclinic* ZrO_2, *no excess phases.*
				Perovskite	Cubic	Wells [24], Wood [16], Shirane and Hoshino [25].
				Perovskite	$CaTiO_3$ type	Naray-Szabo [26].
$CaZrO_3$	.77	1,550	6	**Perovskite**	**Orthorhombic**[c]	**Coughanour, Roth, Marzullo, and Sennett** [5]. *a=5.587, b=8.008, c=5.758 A.*
$CdO:ZrO_2$	.76			Perovskite	$CaTiO_3$ type (*orthorhombic*).	Naray-Szabo [26]. *As many of the compounds listed in this reference do not actually exist,* $CdZrO_3$ *cannot be accepted as a true compound without further experimental evidence.*
$MnO:ZrO_2$	.71	1,400	3	**No 1:1 compound**		**Roth** [9]. *Contains cubic* ZrO_2 *solid solution plus* Mn_3O_4.
$ZnO:ZrO_2$	.69	1,300	3	**No reaction**		**Present work.**
$CoO:ZrO_2$	0.68			No reaction		Dietzel and Tober [51].
$NiO:ZrO_2$	.67			No reaction		Dietzel and Tober [51].
$TiO:ZrO_2$		1,420 (**Helium**)	3	**No 1:1 compound**		**Roth** [9]. *Contains cubic* ZrO_2 *solid solution plus* TiO. *Specimen supplied by F. Brown, Jet Propulsion Lab., Calif. Inst. of Tech.*
$MgO:ZrO_2$	.66	1,515	48	**No 1:1 compound**		**Coughanour, Roth, Marzullo, and Sennett** [5]. *Contains cubic* ZrO_2 *solid solution plus* MgO.
$BeO:ZrO_2$	.56	1,800	0.5	**No reaction**		**Lang, Roth, and Fillmore** [3].
Mixed oxides containing CeO_2						
$BaCeO_3$	0.83	1,450	1	**Perovskite**	**Pseudocubic**	**Present work.** *a=4.387 A.*
		1,525	2	**Perovskite**	**Pseudocubic**	**Present work.** *a=4.387 A. Possibly orthorhombic.*[h]
				Perovskite	$CaTiO_3$ type	Naray-Szabo [26].
				Perovskite	Cubic	Hoffman [52], Wells [24], Wood [16].
$PbO:CeO_2$	.79	1,225	0.5	**No reaction**		**Present work.**
				Perovskite	$CaTiO_3$ type	Naray-Szabo [26]. *Compound probably does not exist.*
$SrCeO_3$	.76	1,525	4	**Perovskite**	**Orthorhombic**[c]	**Present work.** *a=5.986, b=8.531, c=6.125 A.*
				Perovskite	$CaTiO_3$ type	Naray-Szabo [26].
$CaO:CeO_2$	.72	1,525	1	**No reaction**		**Present work.**
				No reaction		Keith and Roy [19].
				Perovskite	$CaTiO_3$ type	Naray-Szabo [26]. *Compound probably does not exist.*
$CdO:CeO_2$	.72			No reaction		Keith and Roy [19].
				Perovskite	$CaTiO_3$ type	Naray-Szabo [26]. *Compound probably does not exist.*
$MgO:CeO_2$	.62	1,300	1	**No reaction**		**Present work.**
				No reaction		Keith and Roy [19].
				Perovskite	$CaTiO_3$	Naray-Szabo [26]. *Compound probably does not exist. Such a compound could only be an antiperovskite structure.*
$BeO:CeO_2$	.53	1,800	0.5	**No compound**		**Lang, Roth, and Fillmore** [3]. *Possibly a solid solution of* BeO *in* CeO_2.

TABLE 2. *Mixed oxides of the type $A^{+2}B^{+4}O_3$*—Continued

Composition	Tolerance factor for perovskite structure[a]	Heat treatment		Structure type	Symmetry	References and discussion
		Temperature (°C)	Time (hr)			
Mixed oxides containing UO_2[i]						
$BaUO_3$	0.82	1,900 (**Argon**)	0.5	**Perovskite**	**Pseudocubic**	**Lang, Knudsen, Fillmore, and Roth** [8]. *a=4.387 A. Similar to* $BaCeO_3$ *with very small splitting of diffraction peaks.*
$SrUO_3$	.75	1,900 (**Argon**)	.5	**Perovskite**	**Orthorhombic**[c]	**Lang, Knudsen, Fillmore, and Roth** [8]. *a=6.01, b=8.60, c=6.17 A.*
$CaUO_3$	.71	1,800 (**Argon**)	.5	**Perovskite**	**Orthorhombic**[c]	**Lang, Knudsen, Fillmore, and Roth** [8]. *a=5.78, b=8.29, c=5.97 A.*
				Rare earth	Cubic	Alberman, Blakely, and Anderson [27].[j]
$MgO:UO_2$	.61	1,800 (**Argon**)	.5	**No reaction**		**Lang, Knudsen, Fillmore, and Roth** [8].
$BeO:UO_2$	.52	1,800 (**Argon**)	.5	**No reaction**		**Lang, Knudsen, Fillmore, and Roth** [8].
Mixed oxides containing ThO_2[k]						
$BaThO_3$	0.80			Perovskite	Cubic[l]	Hoffman [52], Wells [24], Wood [16].
				Perovskite	$CaTiO_3$ type	Naray-Szabo [26].

[a] As the radii given by Ahrens [30] are closer to Pauling radii than to Goldschmidt radii, the values listed for the tolerance factor are, in general, slightly smaller than those calculated by other authors (Keith and Roy [19], Wood [16]), using modified Goldschmidt radii.

[b] Probably only CaO can form a perovskite compound with MnO_2 (Ward, Gushee, McCarrol, and Ridgely [42]). It seems unlikely that $CaMnO_3$ has a simple cubic structure, and it is tentatively left on the border between orthorhombic and pseudocubic types.

[c] This structure is related to cubic perovskite as follows: $a \cong \sqrt{2}a'$, $b \cong 2a'$, $c \cong \sqrt{2}a'$.

[d] Due to the lanthanide contraction, Hf^{+4} has a radius only slightly smaller than Zr^{+4}, and the compounds containing HfO_2 are probably mostly isostructural with the corresponding ZrO_2 compounds.

[e] The pseudotetragonal structure with $c/a<1$ is actually orthorhombic with $a=\sqrt{2}a'$, $b=2\sqrt{2}a'$, and $c=2c'$.

[f] No compounds of the ilmenite structure type have been found with ZrO_2, or, indeed, with any B^{+4} ion larger than Sn^{+4}.

[g] Strong anomaly of the dielectric constant at about 230° C, antiferroelectric below this temperature.

[h] The exact nature of the distortion has not been determined, as the amount of distortion is small. There are definite splits in the diffraction lines as well as excess peaks other than those for a simple cubic structure.

[i] No work has been reported on UO_2 systems with NiO, CoO, Zn O, MnO, CdO, or FeO.

[j] Published X-ray pattern is that of a mixture of UO_2 solid solution and perovskite compound. Pattern published for Ca_2UO_4 is actually the perovskite-type compound.

[k] Perovskites of the following oxides with ThO_2 have been listed by Naray-Szabo [26]: BaO, PbO, SrO, CaO, CdO, and MgO. Of these reported compounds, probably only $BaThO_3$ really exists (Keith and Roy [19]).

[l] Although no ThO_2 compounds were examined in the present work, it seems likely that $BaThO_3$ would have the same type of structure as is found in $BaCeO_3$ and $BaUO_3$.

d. $CaUO_3$

The compound $CaUO_3$ also has a $CaTiO_3$ structure. However, a 50:50 molecular mixture of CaO and UO_2 does not yield an equilibrium perovskite compound. The formation of the perovskite compound in the CaO-UO_2 system takes place only in the presence of excess CaO. This phenomena has been discussed by Alberman, et al. [27] and by Lang, et al. [8]. The perovskite compounds of the type $A^{+2}B^{+4}O_3$ have been assigned a minimum tolerance factor (t) of 0.77 by Keith and Roy [19]. The tolerance factor for the perovskite structure, as described by Goldschmidt [17], is

$$t=\frac{R_A+R_0}{\sqrt{2}(R_B+R_0)},$$

where

t=tolerance factor for perovskite structure,
R_A=ionic radius of larger cation,
R_B=ionic radius of smaller cation,
R_0=ionic radius of oxygen (=1.40 A).

This tolerance factor for $CaUO_3$ is equal to 0.71 and is the only known $A^{+2}B^{+4}O_3$ perovskite-type compound with t considerably less than 0.77. Some Ca^{+2} may actually substitute for U^{+4} in the B position, accompanied by a partial oxidation of U^{+4} to U^{+6}, to give a structural formula $Ca(U_x^{+4}U_{\frac{1}{2}(1-x)}^{+6}Ca_{\frac{1}{2}(1-x)}^{+2})O_3$. Such a structural substitution results in a total increase in the tolerance factor. However, a replacement of 50 percent of U^{+4} by U^{+6} and Ca^{+2} increases the tolerance factor to only 0.726. Thus it can be seen that the lower limit of 0.77 for the tolerance factor in $A^{+2}B^{+4}O_3$ perovskite structures is not absolutely correct.

e. $BaGeO_3$

The ABO_3 silicate compounds cannot form perovskite-type structures, as the silicon ion is much too small, always occurring in tetrahedral coordination. The B ion must occupy an octahedral position with respect to oxygen, even in the most distorted structures, in order to be classified as a perovskite. As the germanium ion is larger than the silicon ion and is known to occur in octahedral coordination, a study was made of the reaction of GeO_2 and various divalent metallic oxides. The only known case of octahedrally coordinated Ge^{+4} is one of the polymorphic forms of GeO_2. GeO_2 can be readily formed in the rutile-type structure by heating the quartz-type polymorph at 700° C and 20,000 psi.[3] An attempt was made to form a titanate-type $BaGeO_3$ (with the germanium ion in octahedral coordination) by heating the pseudowollastonite form to 700° C at 20,000 psi, but no change in the crystal structure was observed. Differential thermal analyses of $BaGeO_3$ indicated a phase transformation at about 340° C.[4]

[3] A specimen of rutile-type GeO_2 was prepared in [this manner by A. Van Valkenburg and E. Bunting of the Bureau staff.

[4] The differential thermal analysis was performed by E. Newman of the Bureau staff.

This phase transformation is apparently very disruptive, as a pressed pellet of $BaO:GeO_2$ results in finely divided white powder of crystalline $BaGeO_3$ when heated to 1,000° C and furnace cooled. A 1-percent addition of Fe_2O_3 to $BaGeO_3$ results in an intact ceramic specimen with an entirely different X-ray pattern, which may represent a stabilized form of high-temperature $BaGeO_3$.

4.2. Classification of ABO_3 Compounds Containing Double Oxides of Divalent and Tetravalent Ions

A classification of structure types based on the constituent ionic radii can be made for all the compounds of the $A^{+2}B^{+4}O_3$ type. However, the properties of the solid solutions formed by a mixture of two or more compounds cannot always be correlated by a simple radii classification. In an attempt to explain some of these discrepancies a third property, polarizability of the constituent ions, has been used. It is exceedingly difficult, in the present state of knowledge, to arrive at correct values for the polarizability of a given ion in a given structure type. The values used here have been taken mainly from the results published by Roberts [20, 21] and are listed in table 1. However, as Roberts did not give a value for Cd^{+2}, this ion was assigned a value that would fit the observations of other workers. Both Pauling [28] and Kettelaar [29] indicate that the polarizability of the Cd^{+2} ion in a given structure type is between those of Ba^{+2} and of Sr^{+2}. Therefore, the values given by Kettelaar [29] for Ba^{+2}, Cd^{+2}, and Sr^{+2} were compared, proportionately, to those given by Roberts for the Ba^{+2} and Sr^{+2} ions in the perovskite structure, and a value of approximately 0.56 A^3 was assigned to the Cd^{+3} ion.

A basic division of structure types can be made on a two-dimensional chart of ABO_3 compounds, where the radius of the A^{+2} ion is plotted as the ordinate and the radius of the B^{+4} ion as the abscissa. In figure 1 and table 1, all values of the radii, except for Eu^{+2}, are taken from Ahrens [30] and represent the ionic size for sixfold coordination. As pointed out by Wood [16], a correction for coordination would tend to move boundary lines but not to distort the picture of the basic classification. The value for Eu^{+2} has been taken from Green [31] and corrected for a radius of O^{-2} of 1.40 A. In general, a division can be made between structural types containing large and small A^{+2} ions. The boundary of this division usually falls near a value of 1.0 A, and often the Ca^{+2} (0.99 A) or Cd^{+2} (0.97 A) compounds occur in both structure types. For the carbonates, all compounds containing divalent ions larger than Ca^{+2} have the aragonite structure, whereas those with ions smaller than Ca^{+2} have the calcite structure. In the case of the silicates and germanates, the pseudowollastonite structure type occurs for most of the compounds containing large divalent ions, whereas the enstatite structure is found for the small ions like Mg^{+2} (0.66 A).

Except for the Ba and Sr vanadates described in table 2, all other compounds described in this study

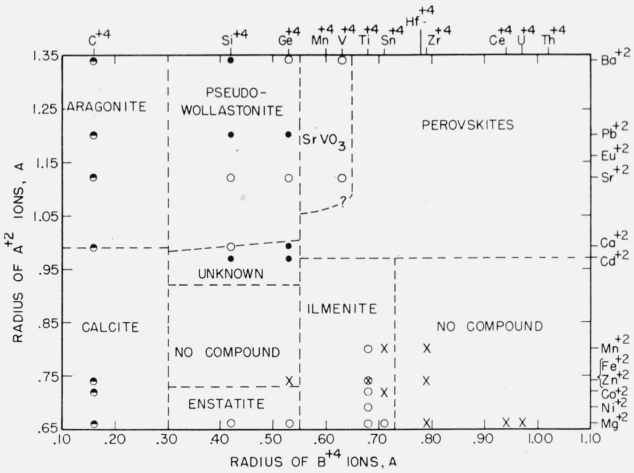

FIGURE 1. *Classification of the $A^{+2}B^{+4}O_3$-type compounds according to the constituent ionic radii.*

○, Compounds studied in the present work that have the structure shown by the areas bounded by dashed lines; ◓, compounds not studied in the present work that are assumed to have the structure shown by the areas bounded by dashed lines; ●, compounds with complex or unknown structure type; ×, position of compositions studied in the present work that do not form $A^{+2}B^{+4}O_3$ compounds; ⊗, the presence of a compound of $FeTiO_3$, and the absence of a compound at the composition $ZnO:TiO_2$ are indicated together, as Zn^{+2} and Fe^{+2} have approximately the same radius.

can be divided into perovskite and ilmenite structure types. The boundary between the two types occurs at a value near that of the Cd^{+2} ion and is shown as horizontal for the purpose of convenience. As no ilmenite compounds are known with a B^{+4} ion larger than the radius of Sn^{+4} (0.71 A), the lower right corner of figure 1 is shown as an area of no compound formation. In all cases the boundary lines between structure types are only an approximation, as not enough information is available on mixtures of compounds of two different structure types. In general, there is only limited solid solution, if any, between compounds of different structure types, although there is considerable or complete solid solution between compounds of a given type. An exception is found in some mixtures of compounds on adjacent sides of the boundary between orthorhombic and cubic (or tetragonal) perovskite compounds.

A classification of those compounds having perovskite-type structures is shown in figure 2. The $A^{+2}B^{+4}O_3$ perovskites can be divided into two general types, those that are cubic or have distortions requiring an elongation of one or more parameters, and those that have distortions that require some multiplication of the basic perovskite unit cell. The latter type is mainly represented by the $CaTiO_3$ orthorhombic structure, those perovskites with relatively larger B^{+4} ions and smaller A^{+2} ions. An intermediate group are those compounds labeled pseudocubic which, although not cubic, have not been definitely identified as to structure type. This group separates the cubic from the orthorhombic perovskites in figure 2. Superimposed upon the cubic group are those compounds that are tetragonal ($c/a>1$) or pseudo-tetragonal ($c/a<1$), ferroelectric and antiferroelectric, respectively. An area showing

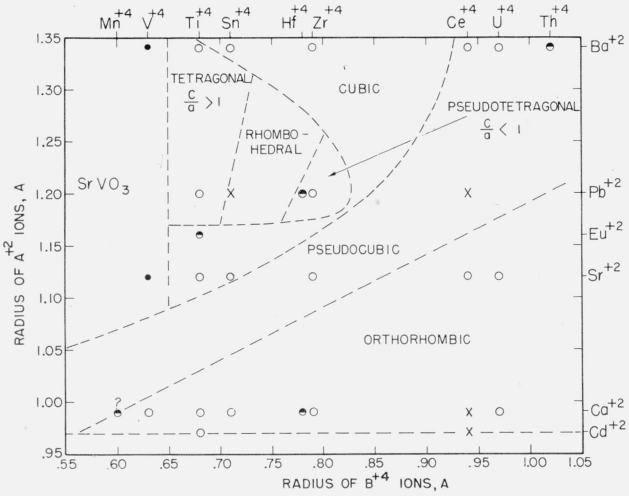

FIGURE 2. *Classification of the perovskite* $A^{+2}B^{+4}O_3$*-type compounds according to the constituent ionic radii.*

○, Compounds studied in the present work that have the structure shown by the areas bounded by dashed lines; ◓, compounds not studied in the present work that are assumed to have the structure shown by the areas bounded by dashed lines; ●, compounds studied in the present work that do not have the perovskite type structure; ×, position of compositions studied in the present work that do not form $A^{+2}B^{+4}O_3$ compounds.

As the compound $CaMnO_3$ has not been studied in the present work and conflicting reports on its symmetry exist, it is tentatively left on the border between orthorhombic and pseudocubic types and is shown by question mark over symbol.

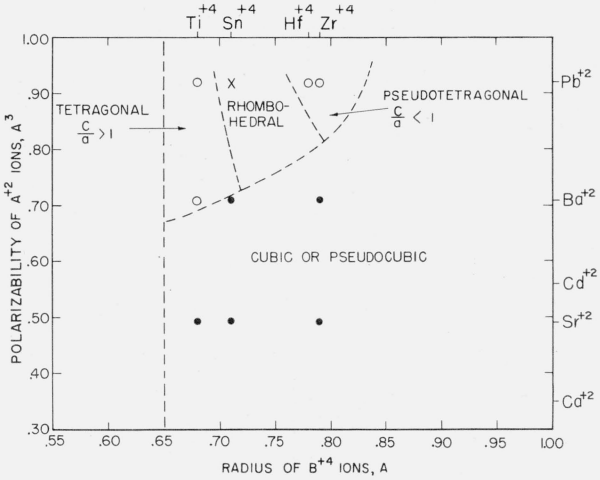

FIGURE 3. *Graph of ionic radii of* B^{+4} *ions and polarizability of* A^{+2} *ions for some of the compounds of the* $A^{+2}B^{+4}O_3$ *perovskite structure type.*

○, Compounds having ferroelectric or antiferroelectric structure types; ●, compounds having cubic or pseudocubic structure types; ×, position of composition that does not form $A^{+2}B^{+4}O_3$ compound.

these compounds can be drawn satisfactorily, as indicated in figure 2. However, if the structures of various solid solutions are discussed in terms of this diagram it is found that there are certain discrepancies in the boundaries of the ferroelectric field. It is true that a complete series of solid solutions exist between $BaTiO_3$ and $PbTiO_3$, all of which are ferroelectric-tetragonal ($c/a>1$). However, complete solid solution also exists between $BaTiO_3$ and $SrTiO_3$, only in this case the solid solutions revert to cubic symmetry (at room temperature) with a relatively small content of $SrTiO_3$. These properties are in contradiction to the ferroelectric field shown in figure 2. The properties of the solid solutions between $PbTiO_3$, $PbZrO_3$, and $PbHfO_3$ can be explained by introducing a rhombohedral field between the tetragonal fields, figure 2.

The discrepancies can be partially explained by utilizing the theory of polarizability of the ions. Ignoring the polarizability values for the tetravalent ions because not enough values are available to make a decent analysis of the results, a three-dimensional plot can be made with polarizability of the divalent ions as the third coordinate. A partial cross section of this type of diagram is shown in figure 3. In this diagram the polarizability of the divalent ions is plotted against the radius of the tetravalent ions. The diagram correlates the solid solutions of Ba, Pb, and Sr titanates. The rhombohedral field has been so drawn in figures 2 and 3 to indicate the ferroelectric phase observed by Shirane and Hoshino [32, 25] in solid solutions of $PbZrO_3$ and $BaZrO_3$.

The symmetries of the ferroelectric solid solutions can best be seen if a three-dimensional model is constructed with polarizability as the third dimension. A diagrammatic representation of such a three-dimensional model is shown in figure 4. The field of ferroelectricity and antiferroelectricity then becomes a volume instead of an area, and the symmetry of solid solutions is correlated by connecting a straight line between the end-member compounds plotted in three dimensions. This straight-line relationship probably only holds true for solid-solution series that do not cross the cubic-orthorhombic boundary. Other solid-solution series probably can only be shown by a curved line connecting the end-member compounds. It is recognized that the polarizability of the B^{+4} ion also plays an important part in determining the symmetry of a perovskite compound. Theoretically the third dimension should be some weighted average of the polarizability of both the A^{+2} and B^{+4} ions. However, as the exact nature of such an average cannot be calculated at the present time only the values for the divalent ions are used. In figure 2 the area of ferroelectricity and antiferroelectricity, represented by the field of tetragonal ($c/a>1$), rhombohedral and pseudotetragonal ($c/a<1$), can now be considered to be a two-dimensional projection onto a basal plane of a volume of such structures formed by plotting polarizability as the third coordinate.

It should be possible to correlate the solid solutions of other perovskite compounds of this group on the basis of the proposed diagrams. However, it should be remembered that the boundaries shown are only approximate; no account is taken of the polarizability of the B^{+4} ion, and the compounds distant from each other in ionic radii, or whose solid-solution series cross symmetry boundaries, do not necessarily have a linear relationship.

In the system $BaTiO_3$-$CaTiO_3$ [33], the tetragonal solid solution extends further than would be shown by a straight line connecting the two compounds in figures 2, 3, and 4. The reason for this is either that the $BaTiO_3$ position is not shown high enough in the

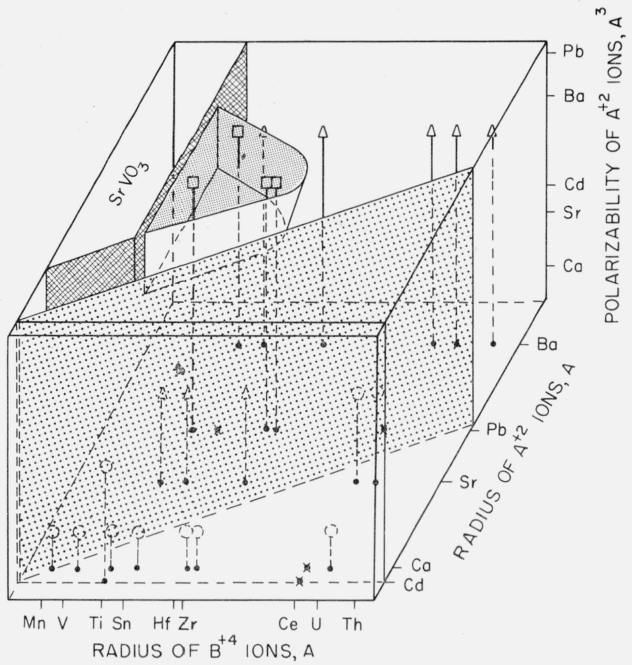

FIGURE 4. *Three-dimensional graph of the perovskite-type* $A^{+2}B^{+4}O_3$ *compounds using ionic radii of the* A^{+2} *and* B^{+4} *ions as two coordinates and the polarizability of the* A^{+2} *ions as the third coordinate.*

○, Position of compounds of the orthorhombic perovskite structure type; △, position of compounds of the cubic or pseudocubic perovskite structure type; □, position of compounds having ferroelectric or antiferroelectric perovskite structure types.

Coarse shading indicates boundary between orthorhombic and pseudocubic structure types; medium shading, boundary enclosing compounds of ferroelectric and antiferroelectric structure types; crosshatch shading, boundary between perovskite and $SrVO_3$ structure types. The boundary between cubic and pseudocubic perovskite types has not been shown on this diagram for the sake of clarity.

field of ferroelectricity because no account is taken of the polarizability of the Ti^{+4} ion, or that the solid-solution symmetries of additions of $CaTiO_3$ to $BaTiO_3$ cannot be shown on a straight-line basis because of the large difference in ionic radii and polarizability. Probably both effects are applicable in this case.

The rhombohedral area has been indicated in figures 2 and 3 because such a symmetry has actually been found in this study. However, the orthorhombic field suggested by McQuarrie and Behnke [33] for the solid-solution series $BaTiO_3$-$BaZrO_3$ and $BaTiO_3$-$CaZrO_3$ has not been included, as the X-ray powder patterns of this orthorhombic phase can only be indexed as pseudocubic and the symmetry is inferred from dielectric data. This orthorhombic field seems very logical and probably should be included somewhere in the diagrams.

McQuarrie [34] has reported a tetragonal phase occurring in the $CaTiO_3$-$SrTiO_3$ system, between 55 mole percent $SrTiO_3$ and 85 mole percent $SrTiO_3$. This tetragonal phase is not shown in figures 2 and 4, although it falls in the pseudocubic area separating the cubic $SrTiO_3$-type structure from the orthorhombic $CaTiO_3$ type. These diagrams predict that, if this system forms a complete series of solid solutions, there should be a field of symmetry other than cubic and orthorhombic. X-ray patterns of specimens prepared by McQuarrie, as well as several prepared in this study, do indeed seem to indicate tetragonal symmetry. However, as $SrZrO_3$, which is also in this pseudocubic area, is definitely not tetragonal, some doubt still exists as to the true symmetry of this portion of the diagram. It is quite likely that all of the area covered by the pseudocubic field in the present diagram does not have the same symmetry. Perhaps the area grades from tetragonal through orthorhombic into still other symmetries. It is apparent that much more work remains to be done on the symmetry of solid solutions of this type before a finished diagram can be presented.

Theoretically figures 2 and 4, especially the three-dimensional diagram (fig. 4), should be usable to predict the symmetries of the solid solutions of any two or more compounds. However, it must be remembered that the positions of the boundaries, as shown, are only approximate because of lack of experimental data on solid solutions. Therefore, at present, the use of figure 4 is limited to selecting the most probable of several possible symmetries. In many cases, several possibilities may seem to be equally probable and experimental evidence will be required before a final decision can be made. The diagram should prove of considerable help in interpreting inconclusive data that might otherwise receive an incorrect or indefinite interpretation.

The present diagrams, figures 2, 3, and 4, have been constructed from the data observed in ceramic bodies at room temperature. The appearance of these diagrams would be quite different if constructed for other temperatures. For instance, at about 500° C the diagrams would show no field of ferroelectric-antiferroelectric compounds and solid solutions. Between −30° C and 0° C $BaTiO_3$ would be orthorhombic instead of tetragonal, and the orthorhombic field, which has been left out in the present diagrams, would play a much more important role in the diagrams. However, at still lower temperatures the rhombohedral symmetry of $BaTiO_3$ would probably increase the area of rhombohedral solid solutions at the expense of the orthorhombic field. It seems certain, however, that if enough information on various compounds and solid solutions were available, a diagram of this sort could be prepared for any given temperature, which would explain the solid solutions of the perovskite compounds at that temperature.

4.3. Mixed Oxides of Trivalent Ions

a. General

Mixed oxides of the trivalent ions are known to form perovskite-type structures [26, 19]. Very recently a patent has been granted B. T. Matthias on an electrical device embodying ferroelectric lanthanum-containing substances. The compound $LaAlO_3$ (and $LaGaO_3$) was claimed to have ferroelectric properties, although no proof of such ferroelectricity or any description of the electrical properties was given [35]. The question as to whether or not these rare-earth aluminates are ferroelectrics is very important. In agreement with single-crystal results of Matthias [35], rather low dielectric con-

stants at room temperature were found for ceramic specimens of relatively high porosity (2 to 4%). The X-ray patterns of these rare-earth aluminates have rhombohedral symmetry, as shown in table 3. The composition, structure type, and symmetry, where known, for the mixed oxides of trivalent ions are listed in table 3. As for table 2, parameters are given only for materials studied in the present work, and results of previous investigations are listed only when controversial subjects are involved or the particular composition has not been studied in the present work.

TABLE 3. *Mixed oxides of the type* $A^{+3}B^{+3}O_3$

Composition	Tolerance factor for perovskite structure[a]	Heat treatment: Temperature (°C)	Heat treatment: Time (hr)	Structure type	Symmetry	References and discussion
Mixed oxides containing Al_2O_3						
$LaAlO_3$	0.94	1,550	5	**Perovskite**	**Rhombohedral** [b]	**Present work.** *a=3.788 A, α=90°4′. Distortion so slight that symmetry is assigned mainly on the basis of comparison with other alumina compounds.*
				Perovskite	$CaTiO_3$ type	Naray-Szabo [26].
				Perovskite	Nearly cubic	Keith and Roy [19].
$CeAlO_3$	.91	1,600 (Helium)	1	**Perovskite**	**Rhombohedral** [b]	**Present work.** *a=3.766 A, α=90°12′.*
				Perovskite	Tetragonal	Zachariasen [53].
				Perovskite	Unknown [c]	Keith and Roy [19].[c]
$NdAlO_3$	.90	1,550	3	**Perovskite**	**Rhombohedral** [b]	**Present work.** *a=3.747 A, α=90°23′.*
				Perovskite	Rhombohedral	Keith and Roy [19].
$SmAlO_3$	.89			Perovskite	Probably rhombohedral.	Keith and Roy [19]. *Probably has same type of structure as* La–Ce *and* $NdAlO_3$.
$Bi_2O_3:Al_2O_3$	.87			Perovskite	Tetragonal [d]	Naray-Szabo [26].
$YAlO_3$	.86	1,550	1	**Perovskite plus garnet**	**Orthorhombic** [e] **plus cubic.**	**Present work.** *Approximately 50 percent of each phase present (perovskite phase, a=5.176, b=7.355, c=5.307 A).*
		1,500	1	**Perovskite plus garnet**	**Orthorhombic** [e] **plus cubic.**	**Present work.** *Amount of perovskite phase has decreased with respect to garnet phase.*
		1,550	19	**Pervoskite plus garnet**	**Orthorhombic** [e] **plus cubic.**	**Present work.** *Amount of perovskite phase has decreased with respect to garnet phase.*
		1,835 [f]	1	**Garnet plus perovskite**	**Cubic plus orthorhombic.**[e]	**Present work.** *Very small amount of perovskite phase present.*
		Low		Garnet solid solution	Cubic	Keith and Roy [19].
		High		$YCrO_3$ type	Tetragonal	Keith and Roy [19]. *Tetragonal* $YCrO_3$*-type structure probably is actually an orthorhombic perovskite structure (see table 4).*
				Perovskite	$CaTiO_3$ type	Naray-Szabo [26].
$In_2O_3:Al_2O_3$	.82			Tl_2O_3 type	Cubic	Keith and Roy [19].
$Fe_2O_3:Al_2O_3$	.76			Corundum	Rhombohedral	Keith and Roy [19].
$Cr_2O_3:Al_2O_3$	.75			Corundum	Rhombohedral	Keith and Roy [19].
$Ga_2O_3:Al_2O_3$	.75			Corundum	Rhombohedral	Keith and Roy [19].
Al_2O_3	.71	1,300	15	**Corundum**	**Rhombohedral**	**Present work.** *a=5.13, α=55°19′.*
Mixed oxides containing Ga_2O_3						
$LaGaO_3$	0.89	1,500	1	**Perovskite**	**Orthorhombic** [e]	**Present work.** *Very slight distortion. a=5.494, b=7.769, c=5.579 A.*
				Perovskite		Keith and Roy [19].
$CeGaO_3$	.86			Perovskite		Keith and Roy [19]. *This compound is probably also orthorhombic.*
$NdGaO_3$	.85	1,500	1	**Perovskite**	**Orthorhombic** [e]	**Present work.** *Distortion greater than in* $LaGaO_3$. *a=5.424, b=7.704, c=5.496 A.*
				Perovskite	Rhombohedral or monoclinic.	Keith and Roy [19].
$Sm_2O_3:Ga_2O_3$	.84			Garnet		Keith and Roy [19]. *Specimen heated to moderate temperature.*
				Unknown		Keith and Roy [19]. *Specimen heated to high temperature.*
$Y_2O_3:Ga_2O_3$	0.81			Garnet		Keith and Roy [19]. *Specimen heated to moderate temperature.*
				Unknown		Keith and Roy [19]. *Specimen heated to high temperature.*
Ga_2O_3	.71			Corundum	Rhombohedral	Keith and Roy [19].
Mixed oxides containing Cr_2O_3						
$LaCrO_3$	0.88			Perovskite	Cubic	Naray-Szabo [26].
				Perovskite		Keith and Roy [19]. "Slight distortion probably monoclinic." *Orthorhombic.*
				Perovskite	Cubic	Wold and Ward [38]. "Possibly very slightly distorted."
				Perovskite	Monoclinic or orthorhombic.	Yakel [43].
$CeCrO_3$	.86			Perovskite	Nearly cubic	Keith and Roy [19].
$NdCrO_3$	.85			Perovskite	Rhombohedral or monoclinic.	Keith and Roy [19]. *Probably orthorhombic.*
$SmCrO_3$	.84			$YCrO_3$ type	Tetragonal	Keith and Roy [19].
$YCrO_3$	.81			Perovskite	Monoclinic	Looby and Katz [36]. *Probably an orthorhombic perovskite of* $CaTiO_3$ *type.*
				$YCrO_3$ type	Tetragonal	Keith and Roy [19]. *All the* $YCrO_3$*-type structures are probably orthorhombic perovskites of* $CaTiO_3$ *type.*
$Fe_2O_3:Cr_2O_3$	.71			Corundum	Rhombohedral	Keith and Roy [19].
Cr_2O_3	.71	As received		**Corundum**	**Rhombohedral**	**Present work.** *a=5.38 A, α=54°50′.*

TABLE 3. *Mixed oxides of the type* $A^{+3}B^{+3}O_3$—Continued

Composition	Tolerance factor for perovskite structure[a]	Heat treatment: Temperature (°C)	Heat treatment: Time (hr)	Structure type	Symmetry	References and discussion
Mixed oxides containing Fe_2O_3						
$LaFeO_3$	0.88	1,500	1	**Perovskite**	**Orthorhombic** [e]	**Present work.** *a=5.545, b=7.851, c=5.562 A.*
				Perovskite	$CaTiO_3$ type	Naray-Szabo [26].
				Perovskite		Keith and Roy [19]. "Very slight distortion, possibly monoclinic." *Orthorhombic.*
				Perovskite	Cubic	W. L. Roth [11], Yakel [43]. *Unit cell twice that of simple perovskite.*
$CeFeO_3$	.86			Perovskite	Probably monoclinic	Keith and Roy [19]. *Orthorhombic*
$NdFeO_3$	.85			$YCrO_3$ type	Tetragonal	Keith and Roy [19]. *Probably orthorhombic perovskite.*
$SmFeO_3$	.83			$YCrO_3$ type	Tetragonal	Keith and Roy [19]. *Probably orthorhombic perovskite.*
$GdFeO_3$	.82			Perovskite	Orthorhombic [e]	Geller [54]. *Same space group listed as given by Megaw* [15] *for* $CaTiO_3$.
$YFeO_3$	.81	1,500	1	**Perovskite**	**Orthorhombic** [e]	**Present work.** *a=5.279, b=7.609, c=5.590 A. Largest distortion from cubic symmetry of any of the perovskites in the present study.*
				$YCrO_3$ type	Tetragonal	Keith and Roy [19]. *All* $YCrO_3$*-type structures are probably orthorhombic perovskites.*
$In_2O_3:Fe_2O_3$	0.77			Tl_2O_3	Cubic	Keith and Roy [19].
Fe_2O_3	.71			Corundum	Rhombohedral	Keith and Roy [19].
Mixed oxides containing Sc_2O_3						
$LaScO_3$	0.82			$YCrO_3$	Tetragonal	Keith and Roy [19]. *Probably orthorhombic perovskite.*
$CeScO_3$	.79			$YCrO_3$	Tetragonal	Keith and Roy [19]. *Probably orthorhombic perovskite.*
$NdScO_3$	.78			$YCrO_3$	Tetragonal	Keith and Roy [19]. *Probably orthorhombic perovskite.*
$Y_2O_3:Sc_2O_3$	.75			Tl_2O_3	Cubic	Keith and Roy [19].
$In_2O_3:Sc_2O_3$	.71			Tl_2O_3	Cubic	Keith and Roy [19].
Sc_2O_3	.71			Tl_2O_3	Cubic	Keith and Roy [19].
Mixed oxides containing In_2O_3						
$LaInO_3$	0.81	1,350	0.5	**Perovskite**	**Orthorhombic** [e]	**Present work.** *a=5.723, b=8.207, c=5.914. A.*
				$YCrO_3$ type	Tetragonal	Keith and Roy [19]. *Probably orthorhombic perovskite.*
				Perovskite	Pseudocubic (orthorhombic).	Padurow and Schusterius [55].
$NdInO_3$	.78	1,350	.5	**Perovskite**	**Orthorhombic** [e]	**Present work.** *a=5.627, b=8.121, c=5.891. A.*
$SmInO_3$	.76	1,350	.5	**Perovskite**	**Orthorhombic** [e]	**Present work.** *a=5.589, b=8.082, c=5.886. A.*
				Tl_2O_3	Cubic	Keith and Roy [19]. *Probably a mistake on the chart as no mention is made of this composition in the text of the paper.*
$Y_2O_3:In_2O_3$	.74			Tl_2O_3	Cubic	Padurow and Schusterius [55].
				Tl_2O_3	Cubic	Keith and Roy [19].
In_2O_3	.71	As received		Tl_2O_3	**Cubic**	**Present work.** *a=10.117. A.*
Oxides of rare-earth type						
$LaYO_3$	0.77			Perovskite	Pseudocubic (orthorhombic).	Padurow and Schusterius [55].
Y_2O_3	.71			Tl_2O_3	Cubic	Keith and Roy [19].
$La_2O_3:Sm_2O_3$	.75			Tl_2O_3	Cubic	Keith and Roy [19].
Sm_2O_3	.71			Tl_2O_3	Cubic	Keith and Roy [19].
Nd_2O_3	.71	As received		**La_2O_3**	**Hexagonal**	**Present work.** *a=3.318, c=5.994. A.*
Ce_2O_3	.71			La_2O_3	Hexagonal	Keith and Roy [19].
La_2O_3	.71	1,200	1	**La_2O_3**	**Hexagonal**	**Present work.** *a=3.405, c=6.132. A.*

[a] Unless otherwise indicated, radii of the ions are taken from Ahrens [30].
[b] This type of rhombohedral distortion of the perovskite structure is similar to that reported by Askhan, Fankuchen, and Ward [37] for $LaCoO_3$.
[c] A symmetrical doublet was reported for the (111) reflection. This doublet was also observed in present work for powdered material; however, intact specimen showed twice the intensity for lower-angle peak, indicating rhombohedral symmetry with $\alpha>90°$.
[d] The structure suggested for $BiAlO_3$ is similar to that of $PbSnO_3$. As the latter compound does not exist, the compound $BiAlO_3$ cannot be accepted without further experimental confirmation.
[e] This structure is related to cubic perovskite as follows: $a\simeq\sqrt{2}a'$, $b\simeq 2a'$, $c\simeq\sqrt{2}a'$.
[f] Temperatures above 1,550° C were obtained by employing a gas-fired commercial furnace capable of practical operation up to about 1,850° C.

b. $YAlO_3$

The compound $YAlO_3$ was assigned to a new structure type, $YCrO_3$, by Keith and Roy [19]. However, the compound $YCrO_3$ has been called a perovskite by Looby and Katz [36]. The X-ray pattern for the $YCrO_3$-type structure in $YAlO_3$ specimens can definitely be indexed as a perovskite type, as can be seen in table 4, and is similar in all respects to the $CaTiO_3$-type structure. This structure has the additional advantage of having a much smaller unit cell. Actually the distortion from a cube is no greater than that found in $CaZrO_3$ or $CaSnO_3$ and does not deserve a new structure-type designation. Therefore, the orthorhombic-type structure, originally assigned to $CaTiO_3$, may now be considered to be the more appropriate structure for the compounds referred by Keith and Roy [19] to the $YCrO_3$ type.

$YAlO_3$ has been reported to form a garnet (solid solution) type structure by Keith and Roy [19] who state that the garnet structure is a low-temperature form and the perovskite ($YCrO_3$) type structure is the high-temperature form. This observation does not agree with the evidence found in the present study (see table 4). A 1:1 mixture of Y_2O_3 and Al_2O_3 heated for 1 hr at 1,500° C contained about 50 percent of the garnet-type structure and 50 percent of the perovskite-type structure. When this specimen was reheated at 1,550° C for 19 hr the amount of the perovskite-type structure had greatly decreased relative to the garnet type. A second specimen of Y_2O_3:Al_2O_3 heated at 1,835° C [5] for 1 hr contained even less of the perovskite structure. It seems that attainment of equilibrium between the garnet and perovskite structures in $YAlO_3$ is a slow process, and one of these structures might be only a metastable phase and have no true equilibrium position. A detailed analysis of the phase equilibria throughout the Y_2O_3-Al_2O_3 system would be necessary to answer this problem completely.

TABLE 4. *X-ray powder diffraction data for* $YAlO_3$

Keith and Roy [19] [a]		Present work [b]			
hkl	*d*	*hkl*	*d* Observed	*d* Calculated	Relative intensity [c]
	A		*A*	*A*	
002	4.24	110	4.23	4.23	11
102	3.70	101	3.70	3.71	34
200	3.68	020	3.68	3.68	22
201	3.36	(Al_2O_3)	-------	-------	------
112	3.32	111	3.31	3.31	23
003	2.89	β121	2.90	-------	5
103	2.67	002	2.65	2.65	24
212	2.62	121	2.61	2.61	100
220	2.59	200	2.59	2.59	32
113	2.51	012	2.50	2.50	12
-----	-----	102	2.38	2.36	5
222	2.22	211	2.220	2.218	8
213	2.16	022	2.154	2.152	21
302	2.12	220	2.082	2.116	9
312	2.05	131	2.048	2.045	9
114	1.996	122	-------	1.99	------
321	1.972	221	-------	1.97	------
204	1.859	202	1.854	1.853	26
400	1.845	040	1.843	1.839	21
214	1.806	032	1.799	1.801	14
331	1.694	-----	-------	-------	------
224	1.655	141	1.651	1.647	10
304	1.640	-----	-------	-------	------
314	1.605	-----	-------	-------	------

[a] This pattern is actually from a specimen of $3Y_2O_3$:$5Al_2O_3$ stated as having the $YCrO_3$ type of structure similar to the 1:1 specimen.
[b] X-ray diffraction lines due to the garnet solid-solution phase have been omitted.
[c] Observed intensity of the difraction peaks relative to the strongest peak.

4.4. Classification of ABO_3 Compounds Containing Double Oxides of Trivalent Ions

As very little is known quantitatively about the polarizability values of the trivalent ions in perovskite compounds, this factor has not been used in the present work to describe the classification of these structures. All the compounds studied are indicated in figure 5 according to the radii of the constituent A and B ions. As a complete diagram would list each compound twice, the B ion, for convenience, is always taken as the smaller ion. It can be seen from this diagram that all of the compounds in the upper left of the diagram, large A^{+3} and small B^{+3} ions, form perovskite-type structures. This group is followed by a belt of Tl_2O_3-type structures, most or all of which probably represent solid solutions rather than true compounds. The lower left corner, containing small ions in both the A and B positions, shows a field of corundum (or ilmenite) type structures, probably solid solutions. The upper-right corner, in which both A and B are large ions, contains a field of La_2O_3-type structures, probably solid solutions rather than compounds. This diagram does not differ appreciably from that of Keith and Roy [19]. However, the perovskite field is enlarged to accept all those compounds classified by Keith and Roy as of the $YCrO_3$ structure. In addition, a line is drawn to separate the field of rhombohedral perovskites from the rest of the perovskite compounds, which apparently all have the $CaTiO_3$-type structure. It should be emphasized here that no compounds of the $A^{+3}B^{+3}O_3$ type are known to have a simple cubic perovskite-type structure.

One discrepancy in figure 5 might be found for the $LaCoO_3$ compound reported by Askhan, Fankuchen, and Ward [37]. Co^{+3} is listed by Ahrens [30] as having a radius of 0.63 A, essentially the same as that of Cr^{+3}. This would place the compound $LaCoO_3$ well within the field of orthorhombic perovskites, instead of in the rhombohedral field as it should be. A possible explanation of this discrepancy, other than assuming incorrect radii or resorting to nonstoichiometry, is the possibility of having large polarizability in the lanthanum cobaltate compound. The compound occurring in the specimen of CeO_2:TiO_2, mentioned earlier, can be explained by this diagram if it is assumed that both Ce^{+4} and Ti^{+4} have been reduced to the trivalent state. Ti^{+3} has a radius of approximately 0.76 A [30] and the compound

[5] Temperatures above 1,550° C were obtained by employing a gas-fired commercial furnace capable of practical operation up to about 1,850° C.

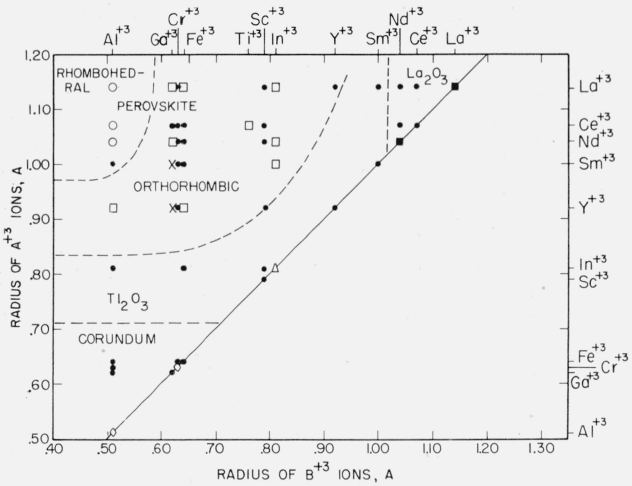

FIGURE 5. *Classification of the* $A^{+3}B^{+3}O_3$*-type compounds according to the constituent ionic radii.*

○, Rhombohedral perovskite, $\alpha > 90°$; □, orthorhombic perovskite ($CaTiO_3$ type); △, Tl_2O_3 structure type; ◇, corundum structure type; ■, La_2O_3 structure type; ●, compounds not studied in the present work that are assumed to have the structure shown by the areas bounded by dashed lines.

$CeTiO_3$ falls well within the field of orthorhombic perovskites, as shown in figure 5. The rare-earth vanadates reported by Wold and Ward [38] can be classified in this grouping as probably orthorhombic, as V^{+3} is listed by Ahrens [30] as having a radius of 0.74 A.

Ferroelectricity in this diagram is represented, possibly, by the $LaAlO_3$ and $LaGaO_3$ compounds. It seems likely that if $LaAlO_3$ is ferroelectric, then all those rare-earth aluminates shown as being rhombohedral are also ferroelectric. It is not known whether any of the other orthorhombic perovskites like $LaGaO_3$ are ferroelectric, but no other reports of ferroelectricity have been found for this type of compound. Assuming, however, that both $LaAlO_3$ and $LaGaO_3$ are ferroelectric [35] and that each has a different symmetry type, a very interesting possibility arises for piezoelectric ceramics. It is known that close proximity to a morphotropic boundary between two ferroelectric solid-solution phases enhances the electrical properties of a ceramic [7]. Therefore, as solid solutions of $LaAlO_3$ and $LaGaO_3$ should cross a morphotropic boundary, interesting piezoelectric properties might be obtained.

5. Summary

The structures of the perovskite compounds of the type $A^{+2}B^{+4}O_3$ can be correlated by plotting a three-dimensional graph with the ionic radii of A^{+2} and B^{+4} as two of the coordinates and the polarizability of the ions as the third dimension. Although it is recognized that the polarizability of both the A and B ions plays an important part in determining the symmetry, only values for the divalent ions have been used. A two-dimensional chart, using only the ionic radii, shows that the perovskite compounds can be divided into orthorhombic and cubic symmetries with a belt of pseudocubic compounds separating the two. Superimposed on the field of cubic compounds is an area of ferroelectric structures. A three-dimensional graph, using the polarizability of the divalent ions as the third dimension, shows that this area is really a projection onto a basal plane of a volume in space encompassing ferroelectric and antiferroelectric compounds and solid solutions.

A two-dimensional plot using ionic radii has also been constructed for double oxides of the trivalent ions. This graph shows perovskite compounds bordered by Tl_2O_3-type structures with corundum and La_2O_3 structures at the extreme borders. The perovskite compounds can be divided into two types. Oxides of the larger rare-earth ions with Al_2O_3 form rhombohedral perovskites with alpha slightly greater than 90°. The rest of the perovskites, including the so-called $YCrO_3$-type compounds, can all be related to an orthorhombic $CaTiO_3$-type structure. No ideal cubic perovskites are found for the $A^{+3}B^{+3}O_3$-type compounds. Ferroelectricity in this graph may be represented by the rhombohedral area and possibly other compounds adjacent to this field.

Thanks are due to L. W. Coughanour and B. Jaffe for providing many of the specimens, to S. Marzullo for measuring their physical properties, to G. F. Rynders for preparing the specimens containing vanadium, and to the staff of the Mineral Products Division of the National Bureau of Standards for many helpful discussions.

6. References

[1] L. W. Coughanour, R. S. Roth, and V. A. DeProsse, J. Research NBS **52,** 37 (1954) RP2470.
[2] B. Jaffe, R. S. Roth, and S. Marzullo, J. Appl. Phys. **25,** 809 (1954).
[3] S. M. Lang, R. S. Roth, and C. L. Fillmore, J. Research NBS **53,** 201 (1954) RP2534.
[4] L. W. Coughanour, R. S. Roth, S. Marzullo and F. E. Sennett, J. Research NBS **54,** 149 (1955) RP2576.
[5] L. W. Coughanour, R. S. Roth, S. Marzullo, and F. E. Sennett, J. Research NBS **54,** 191 (1955) RP2580.
[6] R. S. Roth, Am. Min. **40,** 332 (1955).
[7] B. Jaffe, R. S. Roth, and S. Marzullo, J. Research NBS **55,** 239 (1955) RP2626.
[8] S. M. Lang, F. P. Knudsen, C. L. Fillmore, and R. S. Roth, NBS Circ. 568 (1956).
[9] R. S. Roth, J. Am. Ceram. Soc. **39,** 196 (1956).
[10] P. P. Ewald and C. Hermann, Structurbericht, Z. Krist. (1913–1928).
[11] W. L. Roth, Proceedings of the 12th Annual Pittsburgh Diffraction Conference (1954).
[12] I. Naray-Szabo, Naturwiss. **31,** 466 (1943).
[13] H. D. Megaw, Proc. Phys. Soc. **58,** 133 (1946).
[14] P. Bailey, Thesis, Bristol (1952).
[15] H. D. Megaw, Acta Cryst. **7,** 187 (1954).
[16] E. A. Wood, Acta Cryst. **4,** 353 (1951).
[17] V. M. Goldschmidt, Skrifter Norske Videnskaps-Akad. Mat. Naturvid. Kl. No. 2 (1926).
[18] W. H. Zachariasen, Skrifter Norske Videnskaps-Akad. Mat. Naturvid. Kl. No. 4 (1928).
[19] M. L. Keith and R. Roy, Am. Min. **39,** 1 (1954).
[20] S. Roberts, Phys. Rev. **76,** 1215 (1949).
[21] S. Roberts, Phys. Rev. **81,** 865 (1951).
[22] R. C. Evans, An Introduction to Crystal Chemistry (Cambridge Univ. Press, London, 1948).
[23] E. Posnjak and T. F. W. Barth, Z. Krist. **88,** 271 (1934).
[24] A. F. Wells, Structural Inorganic Chemistry (Oxford Univ. Press, Amen House, London, 1950).

[25] G. Shirane and S. Hoshino, Acta Cryst. **7,** 203 (1954).
[26] I. Naray-Szabo, Müegyetemi Közlemenyek **1,** 30 (1947).
[27] K. B. Alberman, R. C. Blakely, and J. S. Anderson, J. Chem. Soc. (London) **26,** 1352 (1951).
[28] L. Pauling, Proc. Roy. Soc. (London) [A] **114,** 181 (1927).
[29] J. A. A. Ketelaar, Chemical Constitution (Elsevier Publishing Co., Amsterdam, 1953).
[30] L. H. Ahrens, Geochim. Cosmochim. Acta **2,** 155 (1952).
[31] J. Green, Bul. Geol. Soc. Am. **64,** 1001 (1953).
[32] G. Shirane and S. Hoshino, Phys. Rev. **86,** 248 (1952).
[33] M. McQuarrie and F. W. Behnke, J. Am. Cer. Soc. **37,** 539 (1954).
[34] M. McQuarrie, J. Am. Cer. Soc. **38,** 44 (1955).
[35] B. T. Matthias, U. S. Patent Office No. 2,691,738 (1955).
[36] J. T. Looby and L. Katz, J. Am. Chem. Soc. **76,** 6029 (1954).
[37] F. Askhan, I. Fankuchen, and R. Ward, J. Am. Chem. Soc. **72,** 3799 (1950).
[38] A. Wold and R. Ward, J. Am. Chem. Soc. **76,** 1029 (1954).
[39] C. Palache, H. Berman, and C. Frondel, Dana's System of Mineralogy, vol. II (John Wiley and Sons, New York, N. Y., 1951).
[40] A. N. Winchell, Elements of Optical Mineralogy, Pt. II (John Wiley and Sons, New York, N. Y., 1948).
[41] A. Silverman, G. Morey, and F. D. Rossini, Data on chemicals for ceramic use (National Research Council, Washington, D. C., 1949).
[42] R. Ward, B. Gushee, W. McCarrol, and D. H. Ridgely, Univ. Conn. 2d Tech. Rep., NR-052-268, Contract ONR-367(00) (1953).
[43] H. L. Yakel, Acta Cryst. **8,** 394 (1955).
[44] B. W. King and L. L. Suber, J. Am. Cer. Soc. **38,** 306 (1955).
[45] J. Brous, I. Fankuchen, and E. Banks, Acta Cryst. **6,** 67 (1953).
[46] W. W. Coffeen, J. Am. Cer. Soc. **36,** 207 (1953).
[47] G. Shirane and R. Pepinsky, Phys. Rev. **91,** 812 (1953).
[48] C. E. Curtis, L. M. Doney, and J. R. Johnson, Oak Ridge Natl. Lab. ORNL-1681 (1954).
[49] E. Sawaguchi, H. Maniwa, and S. Hoshino, Phys. Rev. **83,** 1078 (1951).
[50] E. Sawaguchi, G. Shirane, and Y. Takagi, J. Phys. Soc. Japan **6,** 333 (1951).
[51] A. Dietzel and H. Tober, Ber. deut. Keram. Ges. **30,** 71 (1953).
[52] A. Hoffman, Z. physik. Chem. [B] **28,** 65 (1935).
[53] W. H. Zachariasen, Acta Cryst. **2,** 388 (1949).
[54] S. Geller, Bul. Am. Phys. Soc. **30,** 15 (1955).
[55] N. N. Padurow and C. Schusterius, Ber. deut. Keram. Ges. **32,** 292 (1955).

WASHINGTON, May 22, 1956.